Differential Effect of B Lymphocyte–induced Maturation Protein (Blimp-1) Expression on Cell Fate during B Cell Development

By Eric J. Messika,* Peter S. Lu,‡§ Yen-Jen Sung,‖ Tony Yao,‡
Jen-Tsan Chi,* Yueh-hsiu Chien,‡ and Mark M. Davis*‡

From the *Howard Hughes Medical Institute, the* ‡*Departments of Microbiology and Immunology
and* §*Department of Dermatology, Stanford University School of Medicine, Stanford, California
94305-5428; and the* ‖*Department of Anatomy, National Yang-Ming University, Taipei,
Taiwan 112, Republic of China*

Summary

The B lymphocyte–induced maturation protein (Blimp-1) upregulates the expression of synde-can-1 and J chain and represses that of c-myc. We have transfected Blimp-1 into two sublines of the BCL1 B cell lymphoma that represent distinct stages of B cell development in secondary lymphoid tissues. After interleukin (IL)-2 and IL-5 stimulation, the BCL1 3B3 cells differentiate into centrocyte-like cells, whereas the BCL1 5B1b cells blast and appear to be blocked at the centroblast stage. This blasting effect and the increase in IgM secretion that follows it can be blocked by a dominant negative form of Blimp-1. At the same time, the ectopic expression of Blimp-1 in these partially activated cells induces an apoptotic response that also can be suppressed by the same dominant negative protein. A similar effect was noticed when Blimp-1 was expressed in the mature L10A and the immature WEHI-231 lines, indicating this may be a general effect at earlier stages of the B cell development, and distinct from the ability of Blimp-1 to induce maturation in late stages of differentiation. Truncation mutants indicate that the induction of the apoptotic response relies mainly on 69 amino acids within Blimp-1's proline-rich domain. We propose that Blimp-1 expression defines a checkpoint beyond which fully activated B cells proceed to the plasma cell stage, whereas immature and partially activated cells are eliminated at this point.

Key words: B lymphocytes • cell differentiation • apoptosis • transcription factors

Differentiation of B lymphocytes into plasma cells depends on their continuous exposure to prodifferentiation and antiapoptosis signals. The majority of nonreactive and self-reactive clones are eliminated in the bone marrow at the pro– (1, 2) and pre–B stages (3). Once mature, the recruitment of new B cells to the long-lived recirculating B cell pool depends on a positive selection process that takes place in the splenic periarteriolar lymphoid sheath (PALS; reference 4). Upon antigen encounter, these long-lived circulating cells are retained in secondary lymphoid organs. After being exposed to the appropriate T cell help, they proliferate and relocate to germinal centers (5), where they are subjected to negative selection before the onset of somatic mutation (6). The surviving cells interact with follicular dendritic cells that supply proliferative, antiapoptotic signals (7, 8) and upregulate the expression of multiple receptors required for T cell interaction (9, 10). The selected B cell clones then interact with T cells that provide them with additional survival signals, induce isotype switching

(11, 12), and aid in their differentiation into plasma or memory cells. Transcription factors that regulate the survival of developing B cells at different points along this pathway remain largely unknown.

We have previously shown that IL-2 and IL-5 upregulate the expression of the B lymphocyte–induced maturation protein (Blimp-1)[1] in mature B cells (13). Blimp-1 and its human homologue PRDI-BF1 (14, 15) are zinc finger proteins that contain four Kruppel-like zinc fingers as well as a number of other domains that may mediate protein–protein interactions (13, 16). Transfection of Blimp-1 into the BCL1 CW13.20-3B3 mature B cell line (hereafter referred to as 3B3) induces IgM secretion, J chain upregula-

tion, and Syndecan-1 expression (13). Blimp-1 has also been shown recently to regulate the expression of c-myc in mature B cells (17). As Blimp-1 is gradually upregulated from the mature B cell stage to the plasma cell (13), the expression of c-myc is progressively turned off (18). During this transition phase, c-myc controls both proliferation and apoptosis (19), depending on signals provided by cytokines (20). Thus, it is likely that Blimp-1 is a component of a regulatory complex that controls the differentiation and apoptosis of activated B cells. In this work, we have identified an apparent temporal window within which Blimp-1 causes apoptosis as opposed to maturation. In particular, we have found that ectopic expression of Blimp-1 in the immature WEHI-231, mature L10A, and partially activated mature BCL1 5B1b cell line, but not in activated 3B3 cells, results in extensive apoptotic death. We have also identified an effector domain responsible for the induction of the apoptotic effect as being mainly composed of a 69-amino acid (aa) stretch that encompasses most of its proline-rich domain. We suggest that Blimp-1 may be a key participant of a regulatory checkpoint that functions to promote fully activated B cells to terminal differentiation and to eliminate partially activated B cells that become arrested along the differentiation pathway.

Materials and Methods

Cell Lines and Cultures

BCL1 3B3 (ATCC CRL 1669) cells were purchased from the American Type Culture Collection (Rockville, MD) and grown as previously described (21). BCL1 5B1b cells were provided by Dr. Samuel Strober (Stanford University) and were grown as previously described (22), except for lowering the concentration of FCS to 10%. Where indicated, IL-2 and IL-5 (10% supernatants from respective IL-2– and IL-5–producing cell lines; reference 23) were added. 18-81 cells were obtained from Dr. Matthias Wabl (UCSF, San Francisco, CA; reference 24), and WEHI 231 1/8 cells from Dr. Noel Warner (Becton Dickinson, San Jose, CA; reference 25). L10A (26) and BAL-17.7.1 (27) cells were a gift of Dr. Richard Asofsky (NIAID, Bethesda, MD). The COS-7 (ATCC CRL 1651) cells were obtained from the American Type Culture Collection (28). Human embryo epithelial cells 293T were provided by Dr. Gary Nolan (Stanford University) and were grown as previously described (29).

Blimp-1 Truncations

Blimp-1 ΔC′. The Blimp-1 open reading frame (ORF) was subcloned into the EcoRI site of the pyDF30 vector (provided by Stephen Ho and Jerry Crabtree, Stanford University), a derivative of the pcD-SRα expression vector (30) that contains a sequence encoding for a flu antigen (FLAG) octapeptide (31) located 3′ from the multiple cloning site. The last 112 aa of Blimp-1 were removed by using a unique Bsp120I site.

Blimp-1 ΔProline. The region encoding for aa 381–450 of Blimp-1 was removed by using the unique AflII and SplI restriction sites in the pyDF30/Blimp-1 vector. The ends of the restriction were blunted and religated, resulting with the generation of an in-frame truncation of 69 aa in Blimp-1 proline-rich domain.

Blimp-1 ΔN′. The XbaI–MspI fragment of the pyDF30/Blimp1 that contains the entire Blimp-1 ORF and flanking sequences was subcloned into the same sites of the pEJM1 vector. This vector was derived from the pSH160s/NFAT vector (provided by Stephen Ho and Jerry Crabtree), and contains a sequence encoding for a FLAG octapeptide followed by three repeats of the SV40 large T antigen nuclear localization signals (NLS) (32). The first 179 aa of Blimp-1's ORF were removed by digesting the pyDF30/Blimp-1 vector with XbaI and XcmI. The resulting construct encoding for an N′ truncated version of Blimp-1 was fused to three repeats of the SV40 NLS and a FLAG tag. This manipulation prevented the deletion of any potential NLS sequences from Blimp-1 NH_2 terminus required for its translocation.

Blimp-1 NZ. Keller and Maniatis (33) found that the 65 aa that located NH_2 terminal to the zinc fingers were important for protein stability. Therefore, we included the equivalent region of Blimp-1 together with its zinc fingers (hereafter named the NZ domain) in the "minimal Blimp-1 protein". Nucleotides 1615–2289 of the Blimp-1 ORF (13) were previously cloned into a pET24d(+) expression vector (Novagene, Madison, WI). In brief, the sequence was amplified for 15 cycles with a high fidelity PCR enzyme (the ULTIMA™DNA polymerase; Roche Molecular Systems, Inc., Branchburg, NJ) and cloned between the BamHI and HinDIII sites of the vector pET24d(+). The NZ fragment was generated from HindIII digestion of the Blimp-1 containing pET24d(+) vector followed by blunting and was then cloned into the EcoRI site of pEJM1 vector.

GFP Expression Vector

The green fluorescent protein (GFP) expression vector was based on the pG310 expression vector provided by Dr. Edward Mocarski (Stanford University). In brief, the promoter and enhancer of ie1, exon 1, and intron 1 of CMV (−1022 to +947) were inserted between the XbaI and HinDIII sites of the polylinker of pGEM-2 (Promega, Madison, WI). A polyadenylation signal from the ie1 gene was inserted between the BamHI and ClaI sites (+2756 to +2916). Finally, the NheI–XbaI portion of the pG310 was removed. A vector containing a mutated GFP ORF (provided by Dr. Stanley Falkow, Stanford University), which produces an enhanced fluorescent protein (34), was blunt-ended and ligated into the EcoRV site of LITMUS™ 28 (New England Biolabs, Beverly, MA). An EcoRI–BamHI fragment that contained the GFP insert was cloned into the same sites of pG310. The resulting GFP expression vector was named pTYG-1.

Transient Transfections

All cells (except 293T) were transfected by electroporation according to Chu et al. (35). BCL1 and COS-7 cells were suspended at 2.5×10^7/ml in DMEM plus 10% FCS. Ten million cells (400 μl) were placed in a 0.4-cm electrode gap gene pulser cuvette (Bio-Rad, Hercules, CA). After the addition of 10 μg of the vector(s), the samples were gently shaken and subjected to electroporation in a GENEPULSER™ apparatus (Bio-Rad) set to 960 μF and 230 mV for COS-7 cells or 250 mV for BCL1 5B1b and 3B3 cells. The cells were then incubated for 10 min at room temperature and resuspended in 10 ml of complete media. Approximately 10% of the cells were plated on a coverslip placed in a 6-well tissue culture dish and used for immunostaining 24 h after transfection. The rest of the cells were plated in a 10-cm dish and incubated for 48 h before lysis and Western blot analysis. 18-81 cells were suspended at 1.7×10^7/ml in RPMI plus 10% FCS. Five million cells (300 μl) were subjected to electroporation set to 960 μF and 240 mV as described above. The transfected cells

were cultured in 10 ml RPMI media for 18 h. WEHI 231 1/8 and L10A cells were suspended at 2×10^7/ml DMEM plus 20% FCS. Five million cells (250 µl) were incubated for 10 min on ice with the vector(s) before being electroporated (960 µF, 240 mV). After electroporation, the cells were kept on ice for 5 min, and then 1.75 ml DMEM plus 20% FCS were added and the suspensions were kept at room temperature for 10 min. The transfected cells were transferred to a 6-well petri dish and cultured for 18 h. 293T cells were transfected by the calcium phosphate method according to Pear et al. (36). In brief, 7.5×10^6 cells were transfected with 5 µg of truncated Blimp-1 expression vectors. 48 h after transfection the cells were harvested and nuclear extracts were prepared.

In situ TUNEL Assay

The TUNEL (TdT-mediated dUTP nick end labeling) assay was performed with an in situ cell death detection kit following the manufacturer's instruction (Boehringer Mannheim GmbH, Mannheim, Germany). In brief, DP1/GFP double transfected and GFP transfected control 3B3 and 5B1b cells were sorted by FACS® (Becton Dickinson) and incubated for an additional 48 h. The cells were then centrifuged onto glass slides using a Shandon cytospin (Pittsburgh, PA), air dried, and fixed for 30 min in 4% paraformaldehyde diluted in PBS (pH 7.4). After permeabilization with 0.1% Triton X-100 diluted in 0.1% sodium citrate, the cells were labeled with 50 µl of the TUNEL reaction mixture for 60 min at 37°C, washed, and incubated for 30 min with 50 µl of converter-alkaline phosphatase. The slides were rinsed and incubated for 10 min at room temperature with 100 µl of Fast Red TR/Naphthol AS-MX solution (Sigma Chemical Co., St. Louis, MO).

Immunostaining

pEJM1/NZ transfected cells were harvested 24 h after plating, fixed with 4% paraformaldehyde, and permeabilized with 0.1% Triton X-100 diluted in PBS. The cells were then stained for 1 h with a mixture of 1% BSA, 2% normal rat serum, and a 1:1,000 dilution of anti-FLAG® M2 antibody (Eastman Kodak Co., Rochester, NY). Cells were then washed with PBS and stained with a 1:1,000 dilution of a biotinylated goat anti–mouse antibody (PharMingen, San Diego, CA) diluted in 1% BSA solution in PBS. The slides were washed again with PBS and stained with 1% BSA and a 1:1,000 dilution of FITC-conjugated avidin diluted in 1% BSA solution in PBS. The cover slips were mounted on slides with 10 µl of VECTASHIELD® (Vector Labs., Inc., Burlingame, CA), fixed with nail polish, and examined under a fluorescence microscope.

FACS® Analysis and Cell Sorting

Cells were stained with mAbs for 30 min on ice in 50 µl of PBS supplemented with 5% FCS (FACS buffer). The stained cells were washed twice in FACS buffer, then resuspended in 200 µl of buffer and analyzed on a FACScan® with the FACSDesk software (Beckman Center Shared FACS® Facility, Stanford University). The antibodies used for the staining were the monoclonal 6A5.1 anti-BCL1 idiotype (gift of Ellen Vitetta, Southwestern Medical Center, Dallas, TX), FITC-conjugated anti-IgD, PE-conjugated anti–B7-2, FITC-conjugated anti-CD40, and biotinylated anti–Syndecan-1 (PharMingen), and biotinylated anti-IgM (Sigma Chemical Co.). Biotinylated antibodies were used as a second step with either PE- or FITC-conjugated avidin (PharMingen). Dead cells were excluded in each analysis by propidium iodide (PI) staining (37). GFP$^+$/PI$^-$ transfected 5B1b cells

were sorted 15–24 h after transfection using a preset compensation of the GFP for the PI channel. Cells were sorted into RPMI media, washed once with media, and cultured with or without stimuli for an additional 48 h.

Electromobility Shift Assay

293T cells transfected with truncated Blimp-1 mutants were used to prepare nuclear extracts (38). In brief, cells were lysed in 0.5% NP-40, 30% sucrose, 25 mM Tris-HCl, pH 7.5, 25 mM KCl, and 7.5 mM MgCl$_2$ supplemented with proteinase inhibitors (leupeptin, pepstatin, PMSF, and aprotinin). The nuclei were spun and rinsed with RSB (10 mM NaCl, 10 mM Tris-HCl, pH 7.5, 10 mM MgCl$_2$), and nuclear proteins were extracted. Nuclei were resuspended first in 200 mM NaCl, 50 mM Tris-HCl, 0.2 mM EDTA, 0.2 mM EGTA, 2 mM MgCl$_2$, 0.5 mM dithiothreitol (DTT), 5% glycerol, and protease inhibitors. Subsequently, an equal volume of buffer composed of 600 mM NaCl, 50 mM Tris-HCl, 0.2 mM EDTA, 0.2 mM EGTA, 2 mM MgCl$_2$, 0.5 mM DTT, 5% glycerol, and protease inhibitors was added. The nuclear protein was extracted with rotation at 4°C for 30 min and spun for 60 min at 100,000 g. The protein concentration was determined using a Bradford assay. 5 µg of each nuclear extract was used for EMSA (electromobility shift assay) (38). In brief, the extracts were mixed with 10^5 cpm of ^{32}P–end-labeled PRFI (CGCGTACAGAAAGGAAAGGACTAG) (17) or PRDI (GT-GAAAGGGAGAAGTGAAAGTGGGAAATTCC) (14) probe, 3 µg poly (dI-dC) in binding buffer (10 mM Tris-HCl, pH 7.5, 1 mM DTT, 1 mM EDTA, 5% glycerol, and 10 µM ZnSO$_4$). After 30 min incubation at room temperature, the reactions were subjected to electrophoresis on a 6% polyacrylamide gel at 180V for 1.5–2 h. Competitors (100×) were incubated for 30 min before the addition of the labeled probe. After separation, the gel was fixed, dried, and exposed for 2 h to a BIOMAX MS film at −80°C (Eastman Kodak Co.).

ELISA

The amount of IgM in the supernatants was quantitated using a sandwich ELISA (39). In brief, 50 µl of a 10 µg/ml solution of goat anti–mouse IgM (Sigma Chemical Co.) was plated on an IMMULON® 4 plate and the plate was incubated for 2 h at 37°C. Excessive antibody solution was removed and 200 µl of 5% BSA in PBS was added to each well and incubated overnight at 4°C. The plate was washed three times with 200 µl of 1% BSA/PBS, and incubated for 2 h at 30°C with 200 µl of decreasing dilutions of culture supernatants that had been centrifuged at 1,000 g to remove remaining cell debris. A standard curve was determined with different concentrations of mouse anti-MOPC104e IgM (Sigma Chemical Co.). The plates were washed three times with 1% BSA/PBS and incubated for 2 h with 50 µl of 1:14,000 dilution of alkaline phosphatase–conjugated goat–anti mouse IgM (Sigma Chemical Co.). After three washes the plates were incubated with 50 µl of SIGMA 104® phosphatase substrate (Sigma Chemical Co.) diluted in zinc-buffer (100 mM Glycine NaOH, pH 10.0, 1 mM ZnSO$_4$, 1 mM MgCl$_2$) until a visible color change was seen. The plates were analyzed using a 96-well plate reader and VMAX software according to the manufacturer's recommendation (Molecular Devices, Menlo Park, CA).

Cell Cycle Analysis

Cell cycle analysis was performed according to a modified protocol for PI staining of cell nuclei (40). In brief, cell pellets were
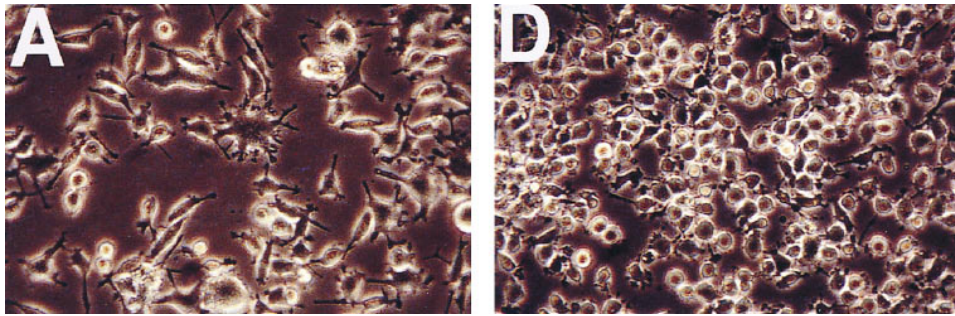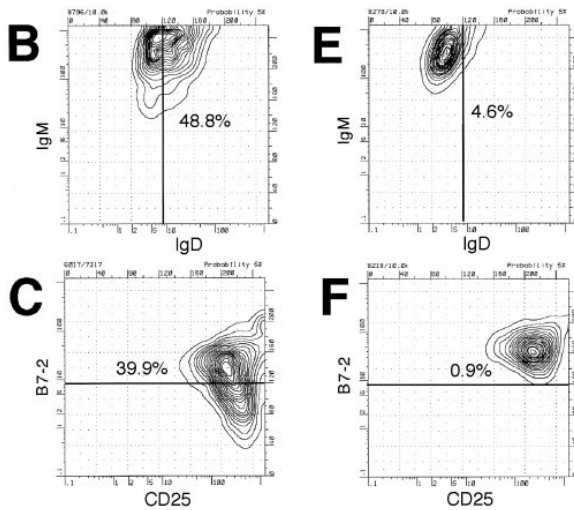
Figure 1. Characterization of BCL1 5B1b and CW13.20-3B3 sublines. Morphology: the BCL1 5B1b (*A*) and CW13.20-3B3 (*D*) sublines were photographed at the log phase at ×320. Expression of cell surface markers: 10^6 cells were stained for 30 min on ice with different combinations of antibodies; anti-IgD and anti-IgM (*B* and *E*) and anti-CD25 and anti–B7-2 (*C* and *F*). The cells were analyzed on a FACScan® with the FACSDesk software. Cell cycle analysis: 10^6 BCL1 CW13.20-3B3 (*a*) and BCL1 5B1b (*b*) cells were permeabilized and the nuclei stained with PI. The distribution of the nuclei size between the different phases of the cell cycle was measured using a FACScan® device and the data were analyzed using the ModFit LT™ algorithm. The percentage of the cells at the different phases of the cell cycle are indicated on the top of each phase.
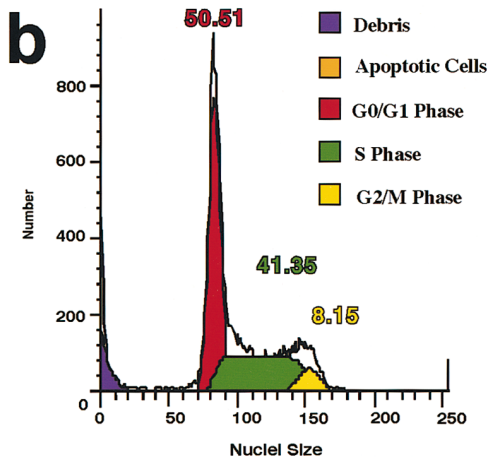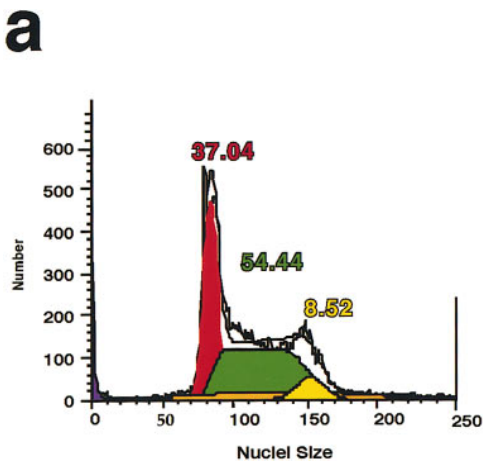
resuspended in 100 μl 85.5 mg/ml sucrose, 11.7 mg/ml sodium citrate, and 5% DMSO, pH 7.6. The cells were trypsinized and permeabilized by adding 900 μl of 0.003% trypsin diluted in SS buffer (0.1% sodium citrate, 0.1% NP-40, 1.5 mM spermine-4HCl in 50 mM Tris base [pH 7.6]) for 20 min. The trypsin and cell RNA were inhibited and degraded by adding 0.05% trypsin inhibitor and 0.01% RNase diluted in SS buffer for 20 min at room temperature. Finally, the cells were stained with 0.01% PI and 3.3 mM spermine-4HCl in SS buffer for 20 min. The cells were then analyzed on a FACScan® or an EPICS® ELITE fluorescense-activated cell sorter (Coulter, Miami, FL) by adjusting the voltage of the instrument to distinguish between the different phases of the cell cycle and data were collected using the FACS-Desk software. The collected data were further analyzed by ModFit® software (Verity Software House, Inc., Topsham, ME) and the distribution of the cells between the different phases of the cell cycle and apoptosis percentages was adjusted to fit the software developer's suggestions.

Results

The 5B1b and 3B3 Sublines Express Surface Markers that Represent Closely Related but Distinct Stages of B Cell Maturation. The mature leukemic 3B3 B cell subline was derived from the leukemia-lymphoma BCL1 5B1b (41) and displays a lower spontaneous secretion level of IgM as compared with the parental line (42). Blackman et al. (21) showed that this low level of secretion is due to deficient J chain expression and suggested that these cells are partially activated due to the lack of a second signaling event for complete maturation. Although the different BCL1 sublines were cloned over a decade ago, the maturation differences between them have not been characterized extensively. When the 5B1b and 3B3 sublines were stained with an antiidiotypic mAb, 6A5.1. (43), both lines were strongly positive (data not shown), confirming that they were derivatives of the same clone. However, they differed in a number of morphological, biochemical, and developmental parameters. The 3B3 line exhibited a more regular and rounded morphology (Fig. 1 *D*) with a slow growth rate.
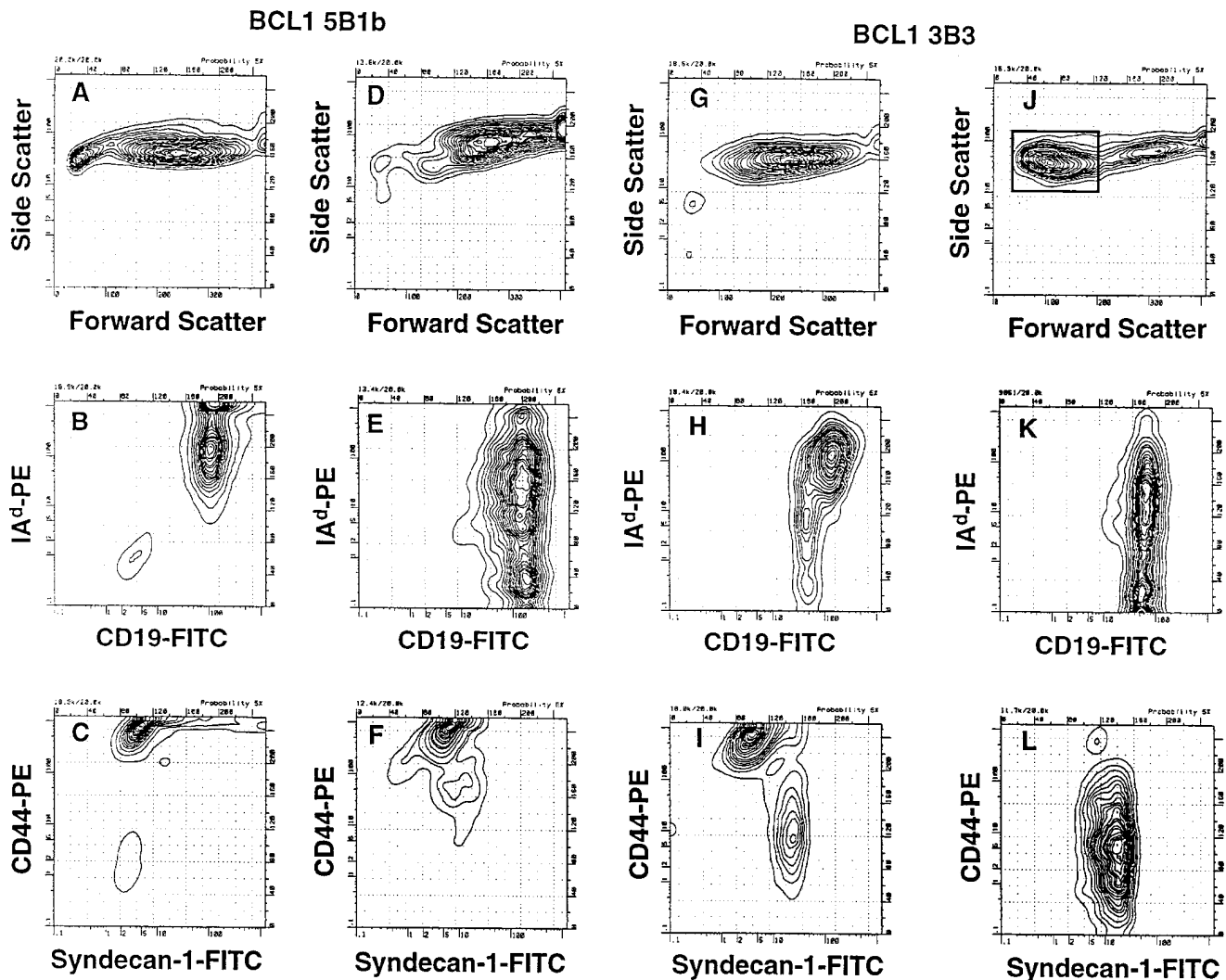
BCL1 5B1b

BCL1 3B3

Figure 2. Kinetics of BCL1 CW13.20-3B3 (*A–F*) and BCL1 5B1b (*G–L*) differentiation after IL-2 and IL-5 stimulation. The two BCL1 sublines were plated at 10^6/ml and stimulated with 10% vol/vol IL-2 and IL-5 supernatants for 72 h. Stimulated (*D–F* and *J–L*) and resting (*A–C* and *G–I*) cells were then collected and subjected to staining with two combinations of markers: anti-IA^d and anti-CD19 (*B, E, H,* and *K*); and anti-CD44 and anti–Syndecan-1 (*C, F, I,* and *L*). The cell size and granularity (*A, D, G,* and *J*) and expression levels of the different markers were measured by a FACScan® device and the data were processed using the FACSDesk software. The expression level of the cell surface markers of BCL1 CW13.20-3B3 at 72 h refers to the population marked with a square box in the cell size/granularity display (*J*) at the top plot. The analysis of the expression of the markers at the other time points refer to the entire cell population.

Cell cycle distribution of the line was characteristic of relatively differentiated cells, with >50% cells in the G0/G1-phase (Fig. 1 *b*). The 5B1b cells, on the other hand, were larger and more dendritic (Fig. 1 *A*), and had a majority (54.4%) of cells in the S-phase of the cell cycle (Fig. 1 *a*).

In addition to these differences in morphology and cell cycle distribution, the expression of several cell surface markers also differed. 40–50% of the 5B1b line exhibited a relatively nonactivated phenotype (IgM^{Bright}IgD^{Bright}CD86^{Dull}) (Fig. 1, *B* and *C*), whereas the 3B3 line appeared to be fully activated (IgM^{Bright}IgD^{Dull}CD86^{Bright}) (Fig. 1, *E* and *F*). This indicates that although both sublines originated from the same mature B cell clone, they differed from each other in their activation states.

3B3, but Not 5B1b Cells, Differentiate into Centrocyte-like Cells after IL-2 and IL-5 Stimulation. Differentiation of the 3B3 cells into IgM secreting cells was characterized by their ability to secrete IgM and upregulate J chain expression (44). We followed the changes in the size and expression of several surface expression markers for 72 h after stimulation with IL-2/IL-5. Before cytokine treatment, the partially activated 5B1b cells were IA^d ^{Bright}CD19^{Bright}CD44^{Bright} Syndecan^{Neg} (references 10, 45; Fig. 2, *B* and *C*), with a cell size peaking at 240 afU (arbitrary fluorescence units) and cell granularity at 160 afU (Fig. 2 *A*). After 72 h of IL-2/IL-5 stimulation, the cell size increased slightly and peaked at 280 afU, and granularity increased to 185 afU (Fig. 2 *D*). This change was accompanied by a 100-fold
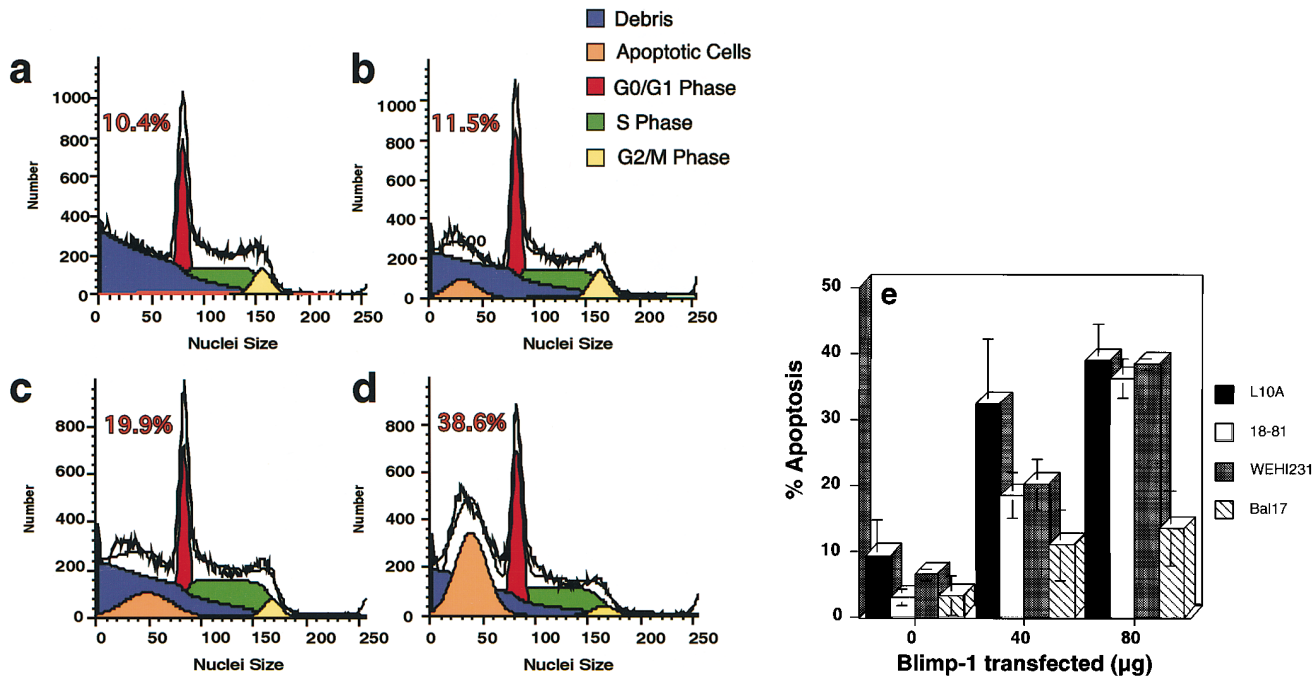
Figure 3. Blimp-1 induces apoptosis in L10A, BAL17, WEHI-231, and 18-81 cells. L10A, WEHI-231, and 18-81 cells were transiently transfected with increasing amounts of the DP1 (Blimp-1) expression vector. After 18 h of recovery at 37°C, the cells were permeabilized and the nuclei stained with PI. The distribution of the nuclei size between the different phases of the cell cycle was measured using an EPICS® Elite fluorescense-activated cell sorter device and the data were analyzed using the ModFIT™ algorithm. Cell cycle analysis of WEHI-231 cells after the transfection of 10 μg (*b*), 40 μg (*c*), 80 μg (*d*), and mock-transfected cells (*a*). The percentage of apoptotic cells is indicated on the top of each transfection. (*e*) Comparison of apoptotic effect of Blimp-1 on WEHI-231, 18-81, BAL17, and L10A cell lines. Cells were transfected with 40 and 80 μg of Blimp-1 and apoptosis was analyzed by cell cycle distribution as described above. The data represent the mean of three experiments (± SEM).

downregulation of IA^d expression on the cell surface of ~30% of the cells (Fig. 2 *E*). There were no noticeable changes in the cell surface expression of CD19, CD44, and Syndecan-1 (Fig. 2 *F*).

In contrast to these relatively minor changes in the 5B1b cells, the 3B3 line responded much more dramatically to IL-2/IL-5 stimulation. In particular, a small percentage of the resting 3B3 cells were IA^d ^{Dull}CD44^{Dull}Syndecan1^{Bright} and expressed ~50% less CD19 (Fig. 2, *H* and *I*) than 5B1b. After IL-2/IL-5 stimulation, this minor population gradually became the dominant phenotype (Fig. 2, *K* and *L*) concomitant with a substantial decrease in cell size from a peak at 220 afU to a peak at 100 afU (Fig. 2, *G* and *J*). These changes suggest that the 3B3 cells differentiated from an activated mature phase to a centrocyte-like cell after IL-2/IL-5 stimulation.

Blimp-1 Induces Apoptosis in Multiple B Cell Lines but Not in the BCL1 3B3. Lin et al. (17) demonstrated that Blimp-1 induces apoptosis in the 18-81 pre–B cell line. This effect was shown to correlate with the downregulation of c-myc expression by Blimp-1. Suppression of c-myc was also reported to induce apoptosis in the immature B cell line WEHI-231 (46). These data suggest that Blimp-1 may induce an apoptotic response at several stages of the B cell development. We therefore compared the effect of the transfection of Blimp-1 into the pre–B 18-81, immature WEHI-231, mature L10A, and the BAL17 cell lines. The results showed

that by as early as 18 h after transfection, 10–80 μg of Blimp-1 induced 11–38% apoptosis in WEHI-231 in a dose-dependent manner (Fig. 3, *a–d*). A similar effect was also found in the L10A and the 18-81 cell lines (Fig. 3 *e* and reference 17). In BAL17, Blimp-1 transfection induced apoptosis but the effect was not dose dependent (Fig. 3 *e*). We also compared the long-term effect of the transfection of a low amount of Blimp-1 into 5B1b and 3B3 cells. Both sublines were transfected with 10 μg of Blimp-1 and 10 μg of GFP constructs, and selected for GFP expression by FACS® after a 15 h incubation. Approximately 5–20% of the cells were positive for GFP, and these were cultured for an additional 72 h and then centrifuged onto slides for in situ TUNEL assay. Apoptosis as determined by the intense nuclear TUNEL staining and condensed nuclear morphology were clearly evident in Blimp-1–transfected 5B1b (Fig. 4 *B*) but not 3B3 (Fig. 4 *A*).

The Blimp-1 "Death Domain" Is Located within the Proline-rich Domain. To identify the domain(s) in Blimp-1 that was involved in the induction of apoptosis, we examined the proapoptotic ability of four truncation mutants in WEHI-231 cells. In the ΔN′ truncation mutant, the N′ acidic domain (aa 71–87) and the first 49 aa of the PRD1-BF1-RIZ homology (PR) domain (aa 131–179) were removed. To compensate for the possible depletion of a necessary NLS, three SV40 NLS were introduced 5′ to the truncated ORF. The results show that this truncation had
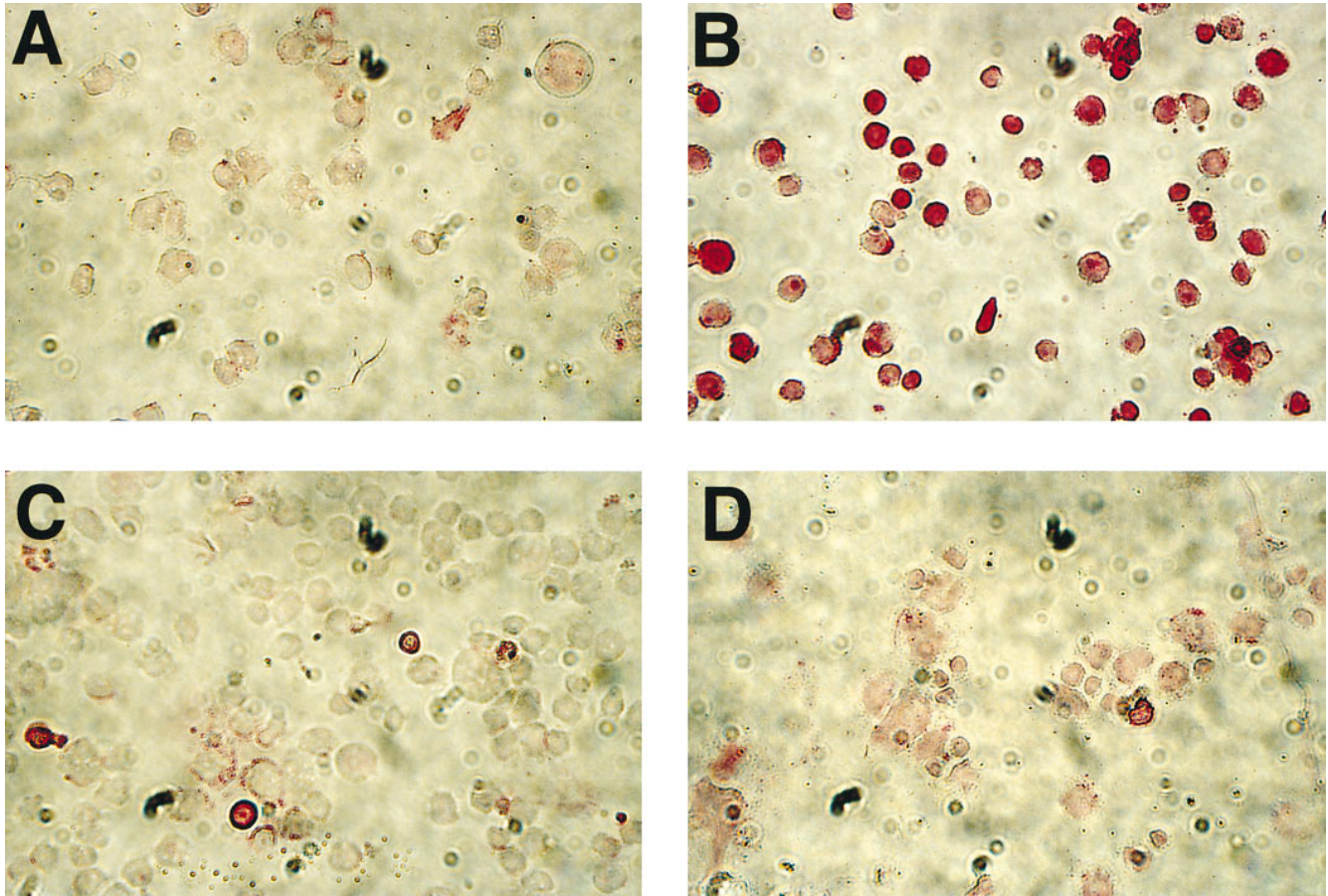
Figure 4. Blimp-1 induces apoptosis in BCL1 5B1b but not in BCL1 CW13.20-3B3 cells. BCL1 5B1b and BCL1 3B3 cells were transiently transfected either with the DP-1 (Blimp-1) vector and the pTYG-1 (GFP) vectors (*A* and *B*) or with the GFP vector alone as a negative control (*C* and *D*). GFP$^+$/PI$^-$ cells were sorted 15 h after transfection and incubated for an additional 48 h. The cells were then cytospun on slides coated with poly-1-lysine, fixed with 4% paraformaldehyde, permeabilized, and stained for in situ TUNEL assay following the manufacturer's instructions. The stained cells were developed with Fast Red and photographed at ×320.

minimal effect on the ability of Blimp-1 to induce apoptosis in WEHI-231 cells (Fig. 4). On the other hand, the depletion of the C′ acidic domain (aa 752–810) had a modest effect on the ability of Blimp-1 to induce apoptosis in WEHI-231 cells (Fig. 5 *B*). The transfection of this ΔC′ truncation mutant reduced the apoptotic ability of Blimp-1 by ∼20%. The most significant effect on the ability of Blimp-1 to kill WEHI-231 cells was noticed when a portion of the proline-rich domain was removed (aa 381–450). The truncation of this domain reduced the apoptotic ability of Blimp-1 on WEHI-231 by 82%. A comparable loss of the proapoptotic activity was observed when most of the putative effector domains of Blimp-1 were removed, as in the NZ construct. The loss of the proapoptotic activity of NZ construct was not due to its inability to translocate into the nuclei because the fusion of the SV40 NLS to the NZ fragment enables proper nuclear translocation of the protein. In situ staining of transfectants with the M2 anti-FLAG antibodies showed that the protein clearly localized to the nucleus (Fig. 5 *D*). Furthermore, the deletion of a major portion of the proline-rich domain in the Δproline construct did not alter the

DNA binding ability of the recombinant protein to the β-interferon (PRDI) or the c-myc (PRFI) elements (Fig. 5 *C*). A similar pattern was observed when most Blimp-1 effector domains were removed in the NZ truncation mutant (results not shown). These results indicate that the loss of the proapoptotic function in the Δproline and the NZ recombinant proteins was probably due to the inability of these truncated proteins to interact with other nuclear factors that are required for the induction of apoptosis.

Blimp-1 Is Involved in the Induction of Apoptosis and Partial Differentiation of 5B1b Cells. To examine whether or not the NZ recombinant protein was able to block the induction of apoptosis in B cells and the development of Blimp-1–induced changes, such as IgM secretion and blasting, we cotransfected 5B1b cells with different combinations of Blimp-1 and/or the NZ construct and with the GFP expression vector as a selection marker. 24 h after transfection, the viable GFP$^+$ 5B1b cells were sorted and incubated for an additional 48 h with or without IL-2/IL-5 stimulation. At the end of the cell culture, the level of IgM, percentage of blasting (cells gated on forward scatter between
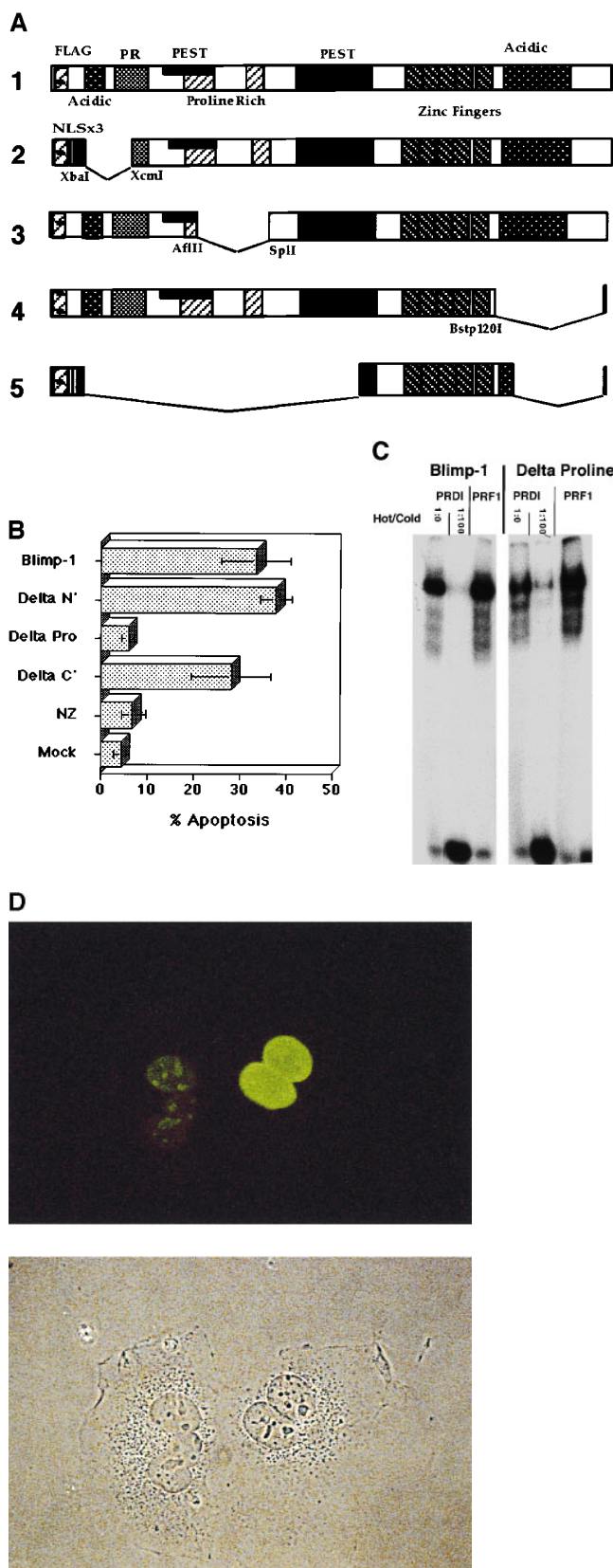
521   Messika et al.

A

FLAG   PR   PEST   PEST   Acidic
1
Acidic   ProlineRich   Zinc Fingers

NLSx3
2
XbaI   XcmI

3
AflII   SplI

4
Bstp120I

5

B

Blimp-1
Delta N'
Delta Pro
Delta C'
NZ
Mock

0   10   20   30   40   50
% Apoptosis

C

Blimp-1   Delta Proline
PRDI   PRF1   PRDI   PRF1
Hot/Cold 1:0 1:100   1:0 1:100

D

Figure 5. Construction, expression, and cellular localization of NZ, a dominant negative form of Blimp-1. (*A*) Scheme of the truncated proteins. Lane *1*, full-length Blimp-1 fused to a FLAG tag; lane *2*, ΔN′; lane *3*, Δproline; lane *4*, ΔC′; lane *5*, NZ. (*B*) Apoptotic efficiency of WEHI-

160 and 250), and percentage of dying cells (determined by GFP^+/PI^+) were examined. The results showed that the transfection of NZ suppressed the low spontaneous cell death of 5B1b. The ectopic overexpression of Blimp-1 induced a robust apoptotic response. This response could be suppressed in cells cotransfected with the NZ and Blimp-1 expression vectors (Fig. 6 *B*). Although insufficient for driving the 5B1b cells to a fully differentiated phenotype (Fig. 2), IL-2/IL-5 treatment induced an increase in IgM secretion and in the percentage of blasts in these cells (Fig. 6 *A*). Ectopic expression of the NZ protein alone resulted in an approximately twofold reduction in both IgM secretion and the percentage of blasting cells in response to IL stimulation (Fig. 6 *A*). However, IL-2/IL-5 treatment of NZ transfected cells produced an apoptotic response that was almost sevenfold higher than control 5B1b cells. On the other hand, Blimp-1 transfection-induced apoptosis of these cells was slightly reduced by IL-2/IL-5 treatment (Fig. 6 *B*). These results suggest that the blasting and IgM secretion effects triggered by IL-2/IL-5 in 5B1b might be dependent on an adequate expression level of Blimp-1. Nevertheless, these effects did not seem to be connected with the apoptotic ability of Blimp-1. Therefore, it seems that in partially activated B cells, Blimp-1 may have a balanced effect between the induction of apoptosis and the induction of maturation. One possible explanation for this effect is that the contribution of Blimp-1 to either pathway requires the coexpression of stage-specific factors that would shift Blimp-1 function from induction of apoptosis to promotion of differentiation.

Discussion

Blimp-1 was originally shown to regulate the expression of structural genes (J chain and Syndecan-1) during the dif-

231 cells after transient transfection with the truncated Blimp-1 proteins. WEHI-231 cells were transiently transfected with 70 μg of the expression vectors expressing the truncated forms of Blimp-1. Mock transfected cells were transfected with 70 μg of the TYG-1 vector. After 18 h of recovery, the cells were harvested and apoptosis was determined by cell cycle analysis. Mean percentage of apoptotic cells was deduced from the cell cycle histograms of three experiments (± SEM), using the ModFit LT™ software according to the software developer. (*C*) EMSA (electromobility shift assay) analysis of Blimp-1 and Δproline. 5 μg of Blimp-1 and Δproline were transfected into 293T cells and nuclear extracts were prepared. 5 μg of the nuclear extracts were used in each gel shift reaction and mixed with labeled PRDI or PRFI probes. PRDI binding competition assays were performed with an excess of 100-fold unlabeled PRDI probe. The reactions were run on a 6% polyacrylamide gel and exposed to an X-ray film for 2 h. (*D*) FLAG tagged NLS-NZ dominant negative protein localize to the cell nuclei (original magnification: ×630). COS-7 cells were transfected transiently with the pEJM1-NZ construct and platted for 15 h on glass coverslip. The adherent cells were fixed with 4% paraformaldehyde and permeabilized with 0.1% Triton X-100/PBS. The cells were then stained with an anti-FLAG M2 antibody (Eastman Kodak Co.), and a sandwich of biotinylated goat anti–mouse antibody (PharMingen) and FITC-conjugated avidin (Amersham International, Little Chalfont, Buckinghamshire, UK). (*D*) Phase contrast view of the transfected cells. Three nuclei are visible on the left cell and two on the right. (*C*) FITC view of the same cells. The nuclei of both cells are stained at different intensities with the anti-FLAG antibody. No staining is visible in the cytoplasmic compartment of the cells.
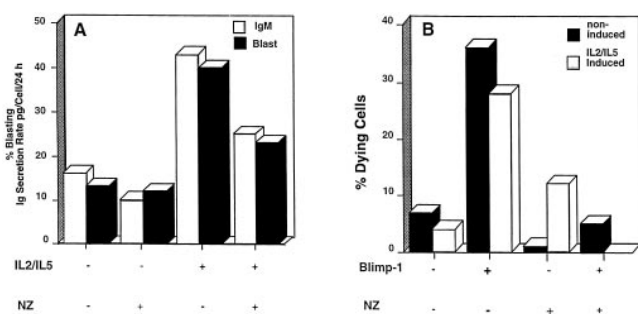
Figure 6. Blimp-1 is involved in the blasting and IgM secretion of BCL1 5B1b after IL-2/IL-5 stimulation but retains its apoptotic ability in uninduced cells. 5B1b cells were transiently transfected with constructs expressing either Blimp-1 (DP1), the dominant negative protein (pEJM1-NZ), or the GFP (pTYG-1) or different combination of these vectors. 24 h after transfection the cells were sorted and either induced for an additional 48 h with 10% IL-2/IL-5 or cultured without induction for the same period. At the end of the incubation period the culture supernatants were collected and assayed for IgM content (*A*) and the cells were analyzed for forward and side scatter after being stained with PI, using a FACStar® device (*B*). The percentage of blasting cells (*black bar*) refers to cells gated with a forward scatter between 160 and 250. Dying cells (*white bar*) were defined as cells positive for both GFP and PI.

ferentiation of mature B lymphocytes into plasma cells (13). Recently, it has been found that the expression of Blimp-1 in pre–B cells triggers an apoptotic response that appears to be mediated by the downregulation of c-myc expression (17). Here we report that Blimp-1 can induce apoptosis across a broad range of immature and mature B cell lymphoma lines and can only promote differentiation in fully activated B cells. We also have identified the functional domain required for the induction of apoptosis and anticipate that Blimp-1 functions may depend upon the stage-specific expression of a cofactor.

The developmental stages represented by the 5B1b and 3B3 sublines appear to define a temporal window of B cell differentiation within which the function of Blimp-1 shifts. Partially activated 5B1b cells are impaired in their responses to IL-2/IL-5 stimulation and arrested at the centroblast stage. On the other hand, fully activated 3B3 cells respond to IL-2/IL-5 stimulation and differentiate into centroblast and, later, centrocyte-like cells (Fig. 2). The transfection of 5B1b cells with the NZ dominant negative suppresses blasting and IgM secretion induced by IL-2/IL-5 treatment (Fig. 6), thus indicating that Blimp-1 is an essential component in IL-2/IL-5 signaling during B cell maturation. In contrast to the antidifferentiation effect of NZ, overexpression of Blimp-1 in 5B1b but not in 3B3 cells results in marked apoptotic death that can be suppressed by the NZ dominant negative. This, in turn, indicates that the Blimp-1–mediated apoptotic machinery is still functional in the 5B1b cells. Similarly, the transfection of Blimp-1 in earlier

stages of the B cell development, such as the pre–B (18-81), immature B (WEHI-231) and mature B (L10A) cell stages induces an apoptotic response. This effect is mainly dependent on a 69-aa region within the proline-rich domain (Fig. 5). It is conceivable that the binding of an additional factor to this domain is required to elicit a response. For example, Blimp-1 may interact in vitro with YY1, a positive regulator of c-myc (17), whose expression plays an important role in controlling the cell fate. Since the downregulation of c-myc was shown to be involved in the induction of apoptosis in both 18-81 (17) and WEHI-231 (46), its suppression by Blimp-1 is anticipated to play a role in the elimination of partially activated B cells. However, it appears that other genes that are involved in the regulation of the cell cycle may be targeted by Blimp-1.

The PR domain (aa 131-231) (16) was suggested to modulate the repressor ability of RIZ (47). Our results show that the deletion of 50% of this domain in the ΔN′ truncated protein had no significant effect on the ability of this protein to induce apoptosis in WEHI-231 cells. Therefore, the integrity of the PR domain may be unnecessary for the induction of apoptosis. In fact, the truncation of either the N′ or C′ acidic domains had only a minor effect on the apoptotic ability of Blimp-1 (Fig. 5 *B*).

Given that Blimp-1 is able to exert such different effects in closely related cells, the question arises as to how this is accomplished. One possible explanation is that different combinations of the zinc finger motifs may recognize distinct gene targets. A mechanism of this type was recently shown in the case of NeP1/CTCF, an 11–zinc finger protein that uses different combination of its zinc fingers to bind to either the c-myc gene or the lysozyme silencer, F1 (48). The partial use of Blimp-1 zinc fingers for the recognition of potential targets was demonstrated in the work of Keller and Maniatis (32). In that report the authors show that two out of the five PRDI-BF1 zinc fingers (and a stretch of 65 aa located N′ to these fingers) are sufficient for its binding to the PRDI element. Recently, we have found that the binding of NZ to the PRF1 element, but not to the PRD1 element, is sensitive to posttranslational modifications or conformational changes (Chi, J.-T., and E.J. Messika, unpublished results). Thus, Blimp-1 may be modulated to switch specificity to different targets due to interactions with stage-specific proteins, using different combinations of its zinc fingers, as the cell matures.

In summary, we propose that Blimp-1 may be part of a "gate keeper" mechanism in the differentiation process, as its upregulation causes apoptosis of immature or partially stimulated B cells. This may constitute an important selection mechanism to eliminate self-reactive B cells that have escaped earlier negative selection mechanisms or have been inappropriately (and partially) activated.

Address correspondence to Mark M. Davis, Howard Hughes Medical Institute, Department of Microbiology and Immunology, Stanford University School of Medicine, Stanford, CA 94305-5428. Phone: 650-723-7962; Fax: 650-723-7771; E-mail: mdavis@cmgm.stanford.edu

References

1. Opstelten, D., and D.G. Osmond. 1983. Pre-B cells in mouse bone marrow: immunofluorescence stathmokinetic studies of the proliferation of cytoplasmic mu-bearing in normal mice. *J. Immunol.* 131:2635–2640.

2. Osmond, D.G. 1990. B cell development in the bone marrow. *Semin. Immunol.* 2:173–180.

3. Nossal, G.J.V. 1994. Negative selection of lymphocytes. *Cell.* 76:229–239.

4. Cook, M.C., A. Basten, and B. Fazekas de St. Groth. 1997. Outer periarteriolar lymphoid sheath arrest and subsequent differentiation of both naive and tolerant immunoglobulin transgenic B cells is determined by B cell receptor occupancy. *J. Exp. Med.* 186:631–643.

5. Nossal, G.J.V. 1994. Differentiation of the secondary B-lymphocyte repertoire: the germinal center reaction. *Immunol. Rev.* 137:173–183.

6. Lebecque, S., O. de Bouteiller, C. Arpin, J. Banchereau, and Y.-J. Liu. 1997. Germinal center founder cells display propensity for apoptosis before onset of somatic mutation. *J. Exp. Med.* 185:563–571.

7. Tew, J.G., J. Wu, D. Qin, S. Helm, G.F. Burton, and A.K. Szakal. 1997. Follicular dendritic cells and presentation of antigen and costimulatory signals to B cells. *Immunol. Rev.* 156:39–52.

8. Lindhout, E., M.L. Mevissen, J. Kwekkeboom, J.M. Tager, and C. de Groot. 1993. Direct evidence that human follicular dendritic cells (FDC) rescue germinal centre B cells from death by apoptosis. *Clin. Exp. Immunol.* 91:330–336.

9. Lenschow, D.J., A.I. Sperling, M.P. Cooke, G. Freeman, L. Rhee, D.C. Decker, G. Gray, L.M. Nadler, C.C. Goodnow, and J.A. Bluestone. 1994. Differential up-regulation of the B7-1 and B7-2 costimulatory molecules after Ig receptor engagement by antigen. *J. Immunol.* 153:1990–1997.

10. Kosco-Vilbois, M.H., D. Gray, D. Scheidegger, and M. Julius. 1993. Follicular dendritic cells help resting B cells to become effective antigen-presenting cells: induction of B7/BB1 and upregulation of major histocompatibility complex class II molecules. *J. Exp. Med.* 178:2055–2066.

11. Lederman, S., M.J. Yellin, A.M. Cleary, A. Pernis, G. Inghirami, L.E. Cohn, L.R. Covey, J.J. Lee, P. Rothman, and L. Chess. 1994. T-Bam/CD40L on helper T-lymphocytes augments lymphokine-induced B cell Ig isotype switch recombination and rescues B cells from programmed cell death. *J. Immunol.* 152:2163–2171.

12. Chin, L.T., A.C. Malmborg, K. Kristensson, J. Hinkula, B. Wahren, and C.A. Borrebaeck. 1995. Mimicking the humoral immune response in vitro results in antigen-specific isotype-switching supported by specific autologous T-helper cells: generation of human HIV-1–neutralizing IgG monoclonal antibodies from naive donors. *Eur. J. Immunol.* 25:657–663.

13. Turner, C.A., Jr., D.H. Mack, and M.M. Davis. 1994. Blimp-1, a novel zinc finger–containing protein that can drive the maturation of B lymphocytes into immunoglobulin-secreting cells. *Cell.* 77:297–306.

14. Keller, A.D., and T. Maniatis. 1991. Identification and characterization of a novel repressor of beta-interferon gene expression. *Genes Dev.* 5:868–879.

15. Huang, S. 1994. Blimp-1 is the murine homolog of the human transcriptional repressor PRDI-BF1. *Cell.* 78:9.

16. Buyse, I.M., G. Shao, and S. Huang. 1995. The retinoblastoma protein binds to RIZ, a zinc-finger protein that shares an epitope with the adenovirus E1A protein. *Proc. Natl. Acad. Sci. USA.* 92:4467–4471.

17. Lin, Y., K.-K. Wong, and K. Calame. 1997. Repression of c-myc transcription by Blimp-1, an inducer of terminal B cell differentiation. *Science.* 276:596–599.

18. Larsson, L.G., M. Schena, M. Carlsson, J. Sallstrom, and K. Nilsson. 1991. Expression of the c-myc protein is down-regulated at the terminal stages during in vitro differentiation of B-type chronic lymphoid leukemia cells. *Blood.* 77:1025–1032.

19. Zornig, M., and G.I. Evan. 1996. Cell cycle: on target with Myc. *Curr. Biol.* 6:1553–1556.

20. Desbarats, L., A. Schneider, D. Muller, A. Burgin, and M. Eilers. 1996. Myc: a single gene controls both proliferation and apoptosis in mammalian cells. *Experimentia.* 52:1123–1129.

21. Blackman, M.A., M.A. Tigges, M.E. Minie, and M.E. Koshland. 1986. A model system for peptide hormone action in differentiation: interleukin 2 induces a B lymphoma to transcribe the J chain gene. *Cell.* 47:609–617.

22. Gronowicz, E.S., C.A. Doss, F.D. Howard, D.C. Morrison, and S. Strober. 1980. An *in vitro* line of the B cell tumor BCL1 can be activated by LPS to secrete IgM. *J. Immunol.* 125:976–980.

23. Karasuyama, H., and F. Melchers. 1988. Establishment of mouse cell lines which constitutively secrete large quantities of interleukin 2, 3, 4 or 5, using modified cDNA expression vectors. *Eur. J. Immunol.* 18:97–104.

24. Wabl, M., J. Meyer, G. Beck-Engeser, M. Tenkhoff, and P.D. Burrows. 1985. Critical test of a sister chromatid exchange model for the immunoglobulin heavy-chain class switch. *Nature.* 313:687–689.

25. Warner, N.L., M.J. Daley, J. Richey, and C. Spellman. 1979. Flow cytometry analysis of murine B cell lymphoma differentiation. *Immunol. Rev.* 48:197–243.

26. Kim, K.J., C. Kanellopoulos-Langevin, R.M. Merwin, D.H.

Sachs, and R. Asofsky. 1979. Establishment and characterization of BALB/c lymphoma lines with B-cell properties. *J. Immunol.* 122:549–554.

27. Mizuguchi, J., W. Tsang, S.L. Morrison, M.A. Beaven, and W.E. Paul. 1986. Membrane IgM, IgD, and IgG act as signal transmission molecules in a series of B lymphomas. *J. Immunol.* 137:2162–2167.

28. Gluzman, Y. 1981. SV40-transformed simian cells support the replication of early SV40 mutants. *Cell.* 23:175–182.

29. Graham, F.L., J. Smiley, W.C. Russell, and R. Nairn. 1977. Characteristics of a human cell line transformed by DNA from human adenovirus type 5. *J. Gen. Virol.* 36:59–74.

30. Takebe, Y., M. Seiki, J.-I. Fujisawa, P. Hoy, K. Yokota, K.-I. Arai, M. Yoshida, and N. Arai. 1988. Srα promoter: an efficient and versatile mammalian cDNA expression system composed of the simian cDNA early promoter and the R-U5 segment of the human T-cell leukemia virus type 1 long terminal repeat. *Mol. Cell. Biol.* 8:466–472.

31. Prickett, K.S., D.C. Amberg, and T.P Hopp. 1989. A calcium-dependent antibody for identification and purification of recombinant proteins. *Biotechniques.* 7:580–589.

32. Goldfarb, D.S., J. Gariepy, G. Schoolnik, and R.D. Kornberg. 1986. Synthetic peptides as nuclear localization signals. *Nature.* 322:641–644.

33. Keller, A.D., and T. Maniatis. 1992. Only two of the five zinc fingers of the eukaryotic transcriptional repressor PRDI-BF1 are required of sequence-specific DNA binding. *Mol. Cell. Biol.* 12:1940–1949.

34. Cormack, B.P., R.H. Valdivia, and S. Falkow. 1996. FACS-optimized mutants of the green fluorescent protein (GFP). *Gene.* 173:33–38.

35. Chu, G., H. Hayakawa, and P. Berg. 1987. Electroporation for the efficient transfection of mammalian cells with DNA. *Nucleic Acids Res.* 12:387–395.

36. Pear, W.S., M.L. Scott, and G.P. Nolan. 1996. Generation of high titre, helper-free retroviruses by transient transfection. *In* Methods in Molecular Medicine: Gene Therapy Protocols. P. Robbins, editor. Humana Press, Totowa, NJ. 41–57.

37. Looken, M.R., and A.M. Stall. 1982. Flow cytometry as an analytical and preparative tool in immunology. *J. Immunol. Methods.* 50:R85–R112.

38. Peterson, C.L., and K. Calame. 1989. Complex protein binding within the mouse immunoglobulin heavy-chain enhancer. *Mol. Cell. Biol.* 7:4194–4203.

39. Harlow, E., and D. Lane. 1988. Immunoassay. *In* Antibodies: A Laboratory Manual. E. Harlow and D. Lane, editors. Cold Spring Harbor Laboratory Press, Cold Spring Harbor, New York. 553–612.

40. Crissman, H.A., and J.A. Steinkamp. 1982. Rapid, one step staining procedures for analysis of cellular DNA and protein by single and dual laser flow cytometry. *Cytometry.* 3:84–90.

41. Slavin, S., and S. Strober. 1978. Spontaneous murine B-cell leukaemia. *Nature.* 272:624–626.

42. Brooks, K., D. Yuan, J.W. Uhr, P.H. Krammer, and E.S. Vitetta. 1983. Lymphokine-induced IgM secretion by clones of neoplastic B cells. *Nature.* 302:825–826.

43. George, A.J.T., A.L. Tutt, and F.K. Stevenson. 1987. Anti-idiotypic mechanisms involved in suppression of a mouse B cell lymphoma, BCL1. *J. Immunol.* 138:628–634.

44. Matsui, K., K. Nakashini, D.I. Cohen, T. Hada, J.I. Furuyama, T. Hamaska, and K. Higashino. 1989. B cell response pathways regulated by IL5 and IL2. *J. Immunol.* 142:2918–2923.

45. Sanderson, R.D., P. Lalor, and M. Bernfield. 1989. B lymphocytes express and lose syndecan at specific stages of differentiation. *Cell Regul.* 1:27–35.

46. Wu, M., M. Arsura, R.E. Bellas, M.J. FitzGerald, H. Lee, S.L. Schauer, D.H. Sherr, and G.E. Sonenshein. 1996. Inhibition of c-myc expression induces apoptosis of WEHI 231 murine B cells. *Mol. Cell. Biol.* 16:5015–5025.

47. Xie, M., G. Shao, I.M. Buyse, and S. Huang. 1997. Transcriptional repression mediated by the PR domain zinc finger gene RIZ. *J. Biol. Chem.* 272:26360–26366.

48. Burcin, M., R. Arnold, M. Lutz, B. Kaizer, D. Runge, F. Lottspeich, G.N. Filippova, V.V. Lobanenkov, and R. Renkawitz. 1997. Negative protein 1, which is required for the function of the chicken lysozyme gene silencer in conjunction with hormone receptor, is identical to the multivalent zinc finger repressor CTCF. *Mol. Cell. Biol.* 17:1281–1288.